PHYSICAL REVIEW B VOLUME 27, NUMBER 4 15 FEBRUARY 1983

Binding energy and electronic structure of small copper particles

B. Delley, D. E. Ellis, and A. J. Freeman
Department of Physics and Astronomy and Materials Research Center, Northwestern University, Evanston, Illinois 60201

E. J. Baerends and D. Post
Department of Chemistry, Free University, Amsterdam, The Netherlands
(Received 15 July 1982)

The equilibrium geometry, binding energy, and electronic structure of small metal particles are investigated using self-consistent one-electron local-density theory. Results for Cu_2, Cu_4, and fcc Cu_{13} and Cu_{79} clusters show an increasing equilibrium bond length with cluster size, and a stiffening of the a_1 vibrational force constants. The calculated binding energies of 1.05 (Cu_2), 1.26 (Cu_4), 2.19 (Cu_{13}), and 3.03 (Cu_{79}) eV/atom compare well with the experimental values of 1.00 (Cu_2) and 3.50 (bulk) eV/atom. For Cu_2 the theoretical bond length and vibrational frequency are found to be in good agreement with experiment. Densities of states and core-level shifts are analyzed to display cluster-size effects. Charge-density maps are used to display the buildup of metallic bonding charge with increasing particle size.

I. INTRODUCTION

The electronic properties of small particles are of interest in many different fields, ranging from the formation and optical properties of interstellar dust grains to the chemistry of smog and dust particles, atmospheric electricity, and nucleation. Recent interest in small metal particles arises because of their important catalytic role in hydrocarbon synthesis reactions as well as in photochemical processes. Further, metallic particles can serve as models for the study of corrosion and reactive properties of rough surfaces. Finally, they also provide models with which to investigate local properties in amorphous and liquid metals.

Noble-metal clusters are particularly interesting since, for metallurgical reasons, good experimental information is available. In addition, Ag particles are catalysts. In contrast to other catalysts the fully occupied d shell simplifies the theoretical treatment.

Experimental studies on small noble-metal particles and thin plates by x-ray diffraction started long ago.[1] These and subsequent studies show that the lattice becomes contracted with decreasing particle size. The same result is obtained from a recent extended x-ray absorption fine-structure (EXAFS) study on supported Cu and Ni particles.[2] In addition, it is observed that the absorption edge shifts to higher binding energy as particle size decreases. X-ray photoemission spectroscopy (XPS) studies of small Ag particles show broadening of the d band and a change in shape with increasing particle size among other structures, which were related to Ag-substrate interactions.[3]

Optical spectroscopy of matrix-isolated Cu atoms and small Cu particles[4] yields information about the electronic level structure. It is observed that clusters containing more than four atoms possess many of the optical features of the bulk metal. Band spectroscopic measurements help to determine the ground state with vibrational modes yielding information about the binding-energy curve and the dissociation energy. Such experiments on Cu_2 have been performed by Ashlund[5] and Kleeman.[6]

There are three basic theoretical approaches available for application to small particles and cluster compounds as follows:

(i) The semiempirical methods, e.g., Hückel, CNDO, and tight-binding linear combination of atomic orbitals (LCAO) schemes.[7] Most particle calculations reported up to now have been performed by semiempirical methods. The Hamiltonian is drastically simplified and the few remaining parameters can be taken from experiment. These methods require calibration against data, which typically are not yet available; thus, very uncertain extrapolations are involved.

(ii) The one-electron self-consistent field methods, e.g., Hartree-Fock (HF) and local-density models.[8] This group of methods does not take input from ex-

periment as a starting point and, in principle, such calculations are carried to self-consistency. Better approximations for the effective electron-electron interaction derived from an underlying many-body theory are continuously sought to obtain more accurate predictions for physical properties. The model Hamiltonian, if treated to sufficient precision, gives an adequate description of *ground-state* properties for many atomic, molecular, and solid-state systems. However, the treatment of excited-state properties is more problematical.

(iii) The many-body methods, e.g., generalized-valence-bond (GVB) and configuration-interaction (CI) methods.[9] In this last group of methods, no approximation is made to the Hamiltonian, in principle, and the wave function is (implicitly or explicitly) of multiple-determinant type. Applications of these GVB and CI methods to transition-metal clusters have been limited because of the greater complexity of the correlated wave function and the large number of configurations involved. Practical limitations on the accuracy of the results also arise from truncation of the single-particle basis set, which is typically made up from Gaussians.

We have developed and applied local-density theory (of which Slater's $X\alpha$ scheme is a special case) for treating spectroscopic and cohesive properties of small particles. The self-consistent one-electron Hamiltonian underlying this theory is

$$h=-\tfrac{1}{2}\nabla^2+V_{\rm eff}(\rho) \tag{1}$$

in Hartree atomic units. $V_{\rm eff}$ contains the classical Coulomb potential arising from the nuclear and electronic charge distributions, as well as exchange and correlation effects. $V_{\rm eff}$ is a functional of the charge density (and of the spin density for open-shell systems), which is represented as a sum over single-particle contributions,

$$\rho=\sum_i f_i\,|\,\psi_i\,|^2\,. \tag{2}$$

The occupation numbers f_i are dictated by the underlying many-body theory. The main simplification for this theory arises from making a local approximation to exchange and correlation effects, thus requiring $V_{\rm eff}$ to be a single-valued function of $\rho(\vec{r})$. It is now well established that this approximation is not severe for homogeneous systems; it cannot be formally justified for inhomogeneous systems such as free atoms.

It is important to realize that wave functions do not play the same role in local-density theory as they do in classical quantum chemical methods. The single-particle orbitals and their eigenvalues are introduced as auxiliary quantities to facilitate determination of the optimum density ρ, which determines the total energy for the lowest state of a given symmetry. The many-body wave function is ill-defined in this theory, since the statistical averaging process mixes different multiplet states of a given configuration. In specific cases it is often possible to project out properties of a particular many-electron state. Furthermore, it is a remarkable fact that the statistical total-energy functional $E(\rho)$ has proved to be useful in determining excited-state properties of atoms, molecules, and solids through application of so-called transition-state theory[8(b)] and through the schemes proposed by Ziegler[10(a)] and by von Barth.[10(b)]

The error in the total energy of atoms calculated from $E(\rho)$ differs typically by less than 1% from (for example) Hartree-Fock (HF) or CI results. This is mostly due to errors in the most highly bound core states, and is traced to the inaccurate treatment of the self-interaction part of the exchange operator. Various Hartree-type modifications of the simple Slater (or Kohn-Sham) potential have been put forward; however, manipulation of nonorthogonal orbitals becomes awkward. The presence of a 1% error in the total energy would be intolerable except for one fact: Here we are interested in the *comparison* of systems where the core states are barely changed. Therefore, core contributions to binding energy will cancel out almost completely. This cancellation is the basis for successful applications of local-density theory in calculating the cohesion of bulk metals.[11]

Small metal particles are mostly open-shell systems. While the density-functional approach is not formally justified for degenerate ground states, it still extrapolates smoothly to an average configuration. This theory underestimates the binding of the lowest multiplet state; however, the result is often still a reasonable approximation. A significant improvement of the theory can be made by allowing $V_{\rm eff}$ to be spin dependent.[12] As in the analogous spin-unrestricted formulation of HF theory, this generalization is sufficient to treat, e.g., singlet-triplet multiplet splittings. Since multiplet splitting is important for determining energies in the isolated-atom case, we find it advisable to treat the reference state of the separated atoms by spin-unrestricted density-functional theory.

II. THEORETICAL-COMPUTATIONAL APPROACH

As the spin-dependent part of the effective potential, we have chosen the so-called $X\alpha$ potential

$$V_{\rm xc}^{\sigma}=-3\alpha\left[\frac{3\rho_{\sigma}}{4\pi}\right]^{1/3} \tag{3}$$

in Hartree atomic units with $\alpha=0.7$ for most of this study. The effective potential has to be determined self-consistently with the charge density for spin direction σ given by

$$\rho_{\sigma}=\sum_{i} f(\epsilon_{i,\sigma})\,|\,\psi_{i,\sigma}\,|^{2}\,. \tag{4}$$

We do not restrict the symmetry of the electron system, and therefore the occupation numbers $f(\epsilon_i)$ are determined by the Fermi-Dirac distribution function.

We have explored two methods of solution to the self-consistent field equations, one using an analytic basis of Slater-type orbitals (STO's) and the other using numerical free-atom—ion wave functions as a variational basis. Such comparisons as can be made are quite useful, since it is possible to verify the numerical accuracy of the computer algorithms and to check on the quality of basis sets required to obtain a given precision.

A. Analytic bases

A conventional STO basis of the form $r^{n}e^{-\zeta r}Y_{lm}(\hat{r})$ located on nuclear sites was used. Applications of this approach to a variety of molecules have been reported in the literature.[13,14] We observed that "double-zeta" basis sets, i.e., roughly two functions per occupied state, are the bare minimum required for quantitative accuracy. We have generally preferred to use "double zeta plus polarization" and "triple-zeta" quality bases in describing transition-metal complexes.

The molecular Coulomb potential is calculated from an analytic least-squares fit to the eigenvector-derived charge density as described previously.[14] The charge-fitting procedure is typically the most tedious step of the calculation since a rather large basis is required to obtain the potential (and hence binding energies) to chemical accuracy.

B. Numerical bases

Basis functions of the form $R_{nl}(r)Y_{lm}(\hat{r})$, with $R_{nl}(r)$ numerical radial functions, were generated with the use of free-atom or ion potentials to localize the functions to nuclear sites. The chief motivation for using numerical bases is to find a compact but accurate representation that can be carried over to many-atom clusters. We observe that satisfactory convergence of valence-electron properties is obtained with two or three radial functions for each l value. Core-electron states are described accurately by a single radial function. In order to describe precisely the dissociation of Cu_n clusters to free Cu atoms, we have included in the basis free atom $3d$, $4s$, and $4p$ functions. In addition, we have included a set of $3d'$, $4s'$, and p' functions generated from free Cu^{+} or Cu^{4+} states to form a "double basis." The one-electron cluster wave functions are obtained in the usual linear variational procedure by solving an energy-independent secular equation determined by a discrete set of sampling points.[14]

Since a major purpose of this study is to extract molecular binding energies and geometries of small particles, we have taken great care to calculate the electrostatic potential accurately. One of the most rapidly convergent representations for the electronic charge density is given by multicenter overlapping multipoles:

$$\rho_{\rm model}=\sum_{i,l,m}\rho_{lm}^{i}(r_i)Y_{lm}(\hat{r}_i)\,. \tag{5}$$

Here i denotes multipoles centered on various nuclear sites at $\vec{r}_i$. A convenient multipolar representation can be obtained from a least-squares fitting procedure with controlled accuracy. The potential can be calculated from this procedure accurately and efficiently.[15] We found sufficient convergence for the copper particles treated here by including multipoles up to $l=2$ in the charge representation.

We recall that the total energy in spin-restricted local-density approximation can be written as

$$\begin{aligned}E_t=&\sum_i \epsilon_i f_i-\tfrac{1}{2}\int\frac{\rho(\vec{r})\rho(\vec{r}\,')}{|\,\vec{r}-\vec{r}\,'\,|}d^3r\,d^3r'\\&+\int\rho(\vec{r})[E_{\rm xc}(\vec{r})-V_{\rm xc}(\vec{r})]d^3r\\&+\tfrac{1}{2}{\sum}'\frac{Z_\mu Z_\nu}{r_{\mu\nu}}\,,\end{aligned} \tag{6}$$

where $E_{\rm xc}(\vec{r})=\frac{3}{4}V_{\rm xc}(\vec{r})$ for the effective potential of Eq. (3). Often the main interest is not in the large total energy, but rather in binding energies with respect to some reference system, e.g., the dissociated molecule

$$E_b=E_t(A)-E_t(B)\,. \tag{7}$$

Binding energies E_b are on the order of a few electron volts, while E_t are on the order of 10^5 eV. It is obvious that numerical noise must be kept under control in order to obtain useful results. Attention

also has to be paid to the computational implementation of Eqs. (6) and (7) so that E_b does not become excessively sensitive to only approximate self-consistency. How this can be achieved is described in more detail in the Appendix. Suffice it to state here that it is possible to calculate E_b to comparable or higher accuracy as that achieved for the individual one-electron eigenvalues.

We note in passing that for the dissociated system Hamiltonian and overlap matrices become diagonal and the eigenvalues of the numerical atomic calculations are recovered. In this respect local-density theory differs greatly from the HF model. It is well known[10(b)] that symmetry-restricted HF wave functions have the wrong dissociation limit, a flaw which can be partially corrected by the use of spin- and orbital-unrestricted single-determinant models. In contrast, the local charge density $\rho(\vec{r})$ displays the correct limiting behavior. However, the *spin density* and its contributions to E_t depend critically upon the presence (or absence) of symmetry restrictions.

III. RESULTS

The free Cu atom contains one unpaired 4*s* electron. Therefore, one could apply the spin-unrestricted formalism of Eq. (3). This gives a total energy of -1638.330 a.u. (1 a.u.$=27.212$ eV); the spin-restricted formalism leads to a 0.0137-a.u. reduction of the total energy. This total energy can be compared to a numerical Hartree-Fock result -1639.964 a.u.,[11] which demonstrates that the local-density approximation leads to relative errors in total energies for atoms of the transition series of order 10^{-3}. As mentioned previously, this error arises mostly from improper cancellation of the self-interaction from the core states. Such errors cancel out in energy comparisons for different geometries of the clusters, which we now proceed to examine.

A. Dimer

1. Analytic basis results

Self-consistent calculations using triple-zeta quality analytic bases have been made on copper particles containing up to nine atoms. The geometry of the bulk metal was used to explore the chemisorption of CO on the CU(001) surface.[16] For the Cu_2 dimer at a (bulk) distance of 4.82 a.u. the binding energy of 2.01 eV was obtained for the $^1\Sigma_g^+$ ground state. Geometry optimization led to a predicted equilibrium bond length of 4.27 a.u., with a binding energy of 2.21 eV and vibrational frequency $\omega_e = 268$ cm^{-1}. These results are in excellent agreement with experiment (see below) and are consistent with the level of accuracy deduced from calculations on smaller closed-shell molecules.[13]

2. Numerical basis results

In order to discover practical limitations of the numerical approach we have investigated the convergence of the binding energy versus the variational basis for the Cu dimer. We include free-Cu-atom functions in the basis, which clearly provide a good starting point for the wave-function expansion at large separation distances. At small bond lengths, additional variational freedom becomes increasingly important. We have chosen a bond length smaller than the equilibrium bond length to investigate the quality of the basis, with results shown in Table I. The first basis chosen (I) consists of Cu 3*d*, 4*s*, and virtual 4*p* atomic functions, while the second (II) contains the 3*d* and 4*s* functions augmented by Cu^{4+}, 3*d*, 4*s*, and 4*p* functions. The third basis (III) uses atomic ground-state *s*,*p*,*d* and Cu^{4+} ionic

TABLE I. Binding energy of Cu_2 at a bond length of $3.5a_0$ vs variational basis quality.

Basis set	*dsp*[a]	$ds+\hat{d}\hat{s}\hat{p}$	$dsp+\hat{d}\hat{s}\hat{p}\hat{f}$
Number of functions	18	30	50
Binding energy (eV/atom)	0.39	0.53	0.55

[a]*dsp* means numerically tabulated atomic functions 3*d*,4*s*,4*p* from a self-consistent atomic $X\alpha$ calculation. The functions $\hat{d},\hat{s},\hat{p}$, are Cu^{4+} numerical functions, and $\hat{d},\hat{s},\hat{p},\hat{f}$ are obtained from a Cu^{4+} ionic state.

s,p,d,f functions. It is evident from Table I that the second basis set considered already yields an almost converged binding energy. It is also interesting to note that inclusion of higher-l components, here an f wave function, barely increases the binding energy. This is in contrast to findings on covalent molecules, where higher-l polarization functions are essential for obtaining accurate basis sets.[17] Not shown in Table I are results for basis sets similar to type II with the additional functions from a Cu^+ ionic calculation. The binding energy coincides with the basis-II result within 10 mV.

Some information about the stability of predicted bond lengths as a function of basis quality was desired, so we have compared binding energies as a function of bond length in Cu_2 for different basis sets. As an example, a comparison for bases II and I is given in Table II. The binding-energy difference between the two bases remains fairly constant at various distances; thus the minimal basis would already have given practically the same binding curve as an accurate basis, but shifted upward in energy. This is rather reassuring, but it should be recalled that our minimal basis set is already capable of giving very accurate results at large distances. Improvement of the basis sets beyond this minimal basis leads then generally to a reduction of equilibrium bond length. Table II suggests that the reduction of bond length versus basis quality is less pronounced than the increase in binding energy. In all calculations reported below we have used basis set II to obtain accurate binding energies.

The ground state for Cu_2 is $^1\Sigma_g^+$. Our theoretical binding energy is 2.10 eV relative to separated, spin-unrestricted atoms. This value is in good agreement with the experimental data of Gingerich[18] (1.99 eV) and Ashlund *et al.*[5] (2.05 eV). From a Morse curve fit to the calculated binding energies between $3.8a_0$ and $5.0a_0$, we deduce a stretch frequency of 286 cm^{-1}. The experimental result of Kleeman and Lundqvist[6] is 266 cm^{-1}. For the equilibrium bond length we obtain $4.20a_0$, which happens to agree precisely with the experimental result of Ashlund *et al.*[5]

3. *Results by other methods*

Previous work by Harris and Jones using density-functional theory in a linear muffin-tin orbital (LMTO) method leads to substantially the same results for Cu_2.[19] As will be shown in Table V, their higher binding energy of 2.30 eV can be traced back to the use of the Gunnarsson-Lundqvist form of the effective potential. In addition to extended Hückel calculations,[20] which yield perfect agreement with experimental data for Cu_2, HF and CI calculations have also been applied to Cu_2 clusters. Joyes and Leleyter[21] find a CI bond length of $r_0=4.16a_0$ and a dissociation energy of $E_b=1.7$ eV. A recent calculation by Bachmann *et al.*[22], using Hartree-Fock theory, yielded $r_0=4.43a_0$ and $E_b=0.84$ eV. Calculations by Noell *et al.*[23] by the generalized-valence-bond method give $r_0=4.66a_0$ and $E_b=0.83$ eV.

B. Tetramer

1. *Analytic basis results*

We have used a triple-zeta STO basis augmented by a single-zeta virtual p set. Computations were done for tetrahedral T_d symmetry at bond lengths of $4.0a_0$, $4.5a_0$, and $5.0a_0$. A parabolic interpolation of the results gives a binding energy of 1.21 eV/atom at a bond length of $4.6a_0$. The configuration found is $^2T_2$ and the one-electron eigenvalue of the highest occupied orbital is -2.43 eV. For comparison, the "surface cluster" with Cu-Cu distance of 4.82 a.u. gave a binding energy of 1.18 eV/atom.[16] The STO calculations thus give a very plausible relaxation of the bond by ~ 0.3 bohr and an increased stabilization of 0.07 eV/atom in passing from the dimer to the tetramer.

2. *Numerical basis results*

Since there has been some controversy about the geometrical shape of transition-metal clusters containing a few atoms, we have calculated the binding

TABLE II. Binding energy (in eV/atom) of Cu_2 at different bond lengths: a comparison of minimal- and extended-basis-set results.

Bond length (bohr)	3.5	4.0	4.5
$E(dsp)$	0.39	0.85	0.85
$E(ds+\hat{d}\,\hat{s}\,\hat{p})$	0.53	1.00	0.99

energy of Cu_4 in linear $D_{\infty h}$, tetrahedral T_d, and distorted tetrahedral C_{2v} symmetry. In any such configuration Cu_4 is found to have a higher binding energy per atom than Cu_2. The tetrahedral geometry of Cu_4 has a predicted binding energy that is slightly higher than the linear Cu_4 chain in the gas phase. It is, however, possible that the linear geometry may be better bound in the solid environment encountered in matrix isolation experiments.[4] We find that the energy difference is only 0.12 eV/molecule in the gas phase, with E_b for the T_d cluster equal to 1.26 eV/atom.

As with the analytic bases we find that tetrahedral Cu_4 is an open-shell $^2T_2$ system; therefore, the spin-unrestricted formalism should be applied. The results of this calculation show that spin-energy contributions are less than 0.01 eV/atom. Jahn-Teller distortions are also expected to occur in the tetrahedral case; however, we find that small distortion in bond lengths (E mode) of $0.1a_0$ contributes less than 0.01 eV to the binding energy. Thus energy gains due to static Jahn-Teller distortions are seen to be small compared to thermal (i.e., room-temperature) energies.

A comparison of results from the numerical and the analytical bases shows that the binding energy is in significantly better agreement than one-electron eigenvalues, which differ by 0.9 ± 0.01 eV. This fact is not surprising since the local-density binding energy is a variational quantity.[24] One-electron eigenvalues are only variational quantities as long as the potential is held fixed. On going to self-consistency a small deviation in the charge density in the low-density region can introduce a dipole barrier that results in an almost uniform shift of all eigenvalues (but not of the dissociation energy). We have investigated the accuracy of the numerical method, which is used for the rest of the present work, in some detail. We find that less than ±0.1-eV error in eigenvalues can be accounted for by truncation of the basis set, less than ±0.1-eV error by truncation of the charge and potential expansion, and less than ±0.05-eV error may be due to inaccuracy of the matrix elements. We also find that the local-density cohesive energy may have been underestimated by 0.05 eV per atom due to limitations in the basis set. Limitations in the charge expansion and approximate numerical integrations lead to a further uncertainty of ±0.05 eV.

C. 13-atom cluster

Cu_{13} is very close to the limits of feasibility for the other *ab initio* methods described in Sec. I, but does not present a major challenge to local-density methods. With the use of the numerical basis approach, we find an electronic ground state with T_{2g} symmetry for the cluster of octahedral symmetry. At an equilibrium nearest-neighbor distance of $4.55a_0$ we find a binding energy of 2.19 eV/atom.

Our findings for the energetics of the Cu_{13} clusters are in disagreement with extended-Hückel-theory calculations,[20] which produce an equilibrium separation of $5.05a_0$ and a 0.78-eV/atom binding energy. We also disagree with recent Hartree-Fock calculations,[22] which find 0.63 eV/atom at an assumed distance of $4.54a_0$ (the equilibrium distance was not calculated).

D. Cu_{79} particle

We have obtained results for Cu_{79} $(=Cu_1Cu_{12}Cu_6Cu_{24}Cu_{12}Cu_{24})$ using the same extended basis set, basis II in Table I, as well as the charge and potential representation used for Cu_{13}. At a fixed nearest-neighbor distance of $4.80a_0$ we find a binding energy of 3.03 eV/atom. The single value of the bond length used was chosen by extrapolation from the smaller clusters toward the bulk value (see below).

This cluster contains six coordination shells and could thus be used to discuss a number of properties as a function of depth from its surface. Let us begin by considering the local density of states (DOS). Discrete partial DOS were calculated for coordination shells by convolution of the level structure with a 0.4-eV full width at half maximum (FWHM) Gaussian and by integration of the orbital densities inside the corresponding atomic spheres,

$$n_{r_1<r<r_2}(\epsilon)=a\sum_i e^{-\alpha(\epsilon-\epsilon_i)^2}\int_{r_1}^{r_2}|\psi_i(\vec{r})|^2 d^3r \ . \tag{8}$$

The surface-atom DOS and the DOS arising from the 19 central atoms are shown in Fig. 1. The surface coordination shells have both a reduced bandwidth and a chemical shift to lower binding energy compared with the central atoms. The narrowing and shift to lower binding energy, which we calculate is in qualitative agreement with the band theory of Appelbaum and Hamann.[25] There are quantitative differences, however, between the DOS at the center of the cluster in the present case and results from bulk and thin-slab calculations, as should be expected. For a cluster with O_h symmetry, the orbital densities all have at least D_{2h} symmetry. Such

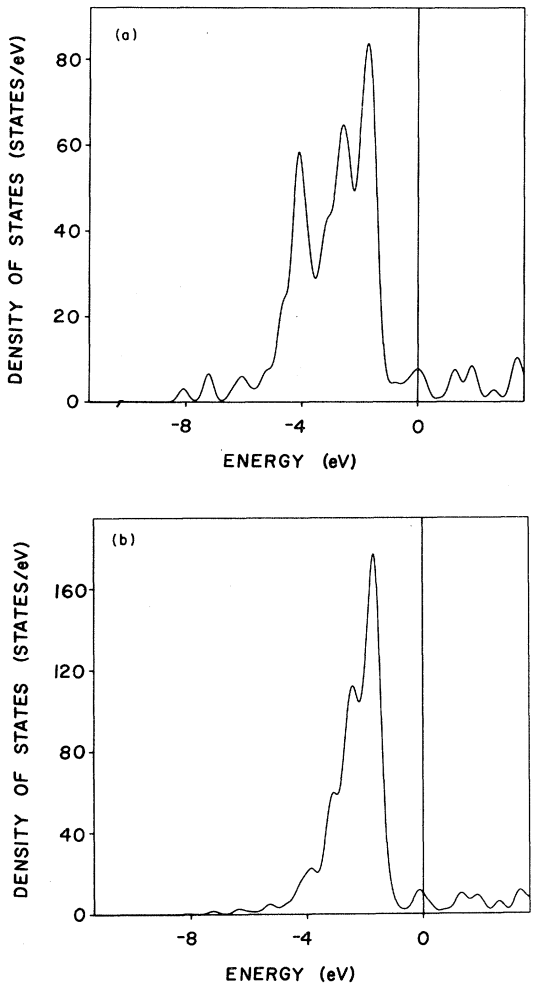

FIG. 1. (a) Partial DOS for a sphere containing the central 19 atoms. The discrete spectrum is convoluted with a Gaussian of 0.4 eV full width at half maximum. (b) Partial DOS for the surface atoms obtained from an integration in a small sphere around each surface atom.

symmetry restrictions for small particles prevent very rapid convergence to bulk DOS, especially at the center atom. For very large clusters bulk DOS would finally be obtained according to a theorem by von Laue,[26] which states that the probability density $\psi^*(r,E)\psi(r,E)$ becomes approximately independent of the form of the boundary condition at distances from the boundary greater than a characteristic length inversely proportional to the wave number.

Next let us discuss core-level shifts at the copper surface compared to interior regions. The simple superposition of atomic charge densities would give rise to a potential giving about 6 eV more binding for the core electrons of the central atom compared to a free atom. However, such an attractive potential near the center of the cluster pulls in a small amount of screening charge, which in turn reduces the core-level shifts. Values for these net chemical shifts (a ground-state property) of ~ 2 eV are shown in Table III. To relate to spectroscopic measurements one has to take into account further energy contributions for the excited-state core-hole screening. We have not performed extensive calculations for this effect so far. For simplicity we assume that screening in the surface shell is as good as it is in the center of the cluster. With this assumption we predict the same relaxation energy for all inequivalent sites. The ground state $\Delta\epsilon_i$ would then predict shifts of 0.4 to 0.8 eV to lower the binding energy of the core levels at the Cu surface. Experimentally unambiguous core-level shifts to 0.5-eV lower binding energy have been found for Au surface atoms.[27].

TABLE III. Core-level shifts for Cu_{79} $2p$ core levels in each coordination shell (in eV). $\Delta\epsilon_i$ is the static shift relative to atomic ground-state value in frozen-core approximation; $\Delta\epsilon_r$ is the shift including both final-state relaxation and screening.

S bulk	$\Delta\epsilon_i$	$\Delta\epsilon_r$
Center atom	−2.14	+ 6.65
2	−2.54	+ 6.25
3	−2.41	+ 6.38
4	−2.14	+ 6.65
5	−1.92	+ 6.87
Surface	−1.73	+ 7.06

Core levels of free atoms are observed at higher binding energy than those for bulk atoms. Here differences in screening for the atom become important. For the free Cu atom the final state is $[\mathrm{Ar}]^{-1}d^{10}s^1$, while in the bulk a screened configuration closer to $[\mathrm{Ar}]^{-1}d^{10}s^2$ would be expected.

A self-consistent atomic calculation shows that the screened $d^{10}s^2$ configuration leads to 8.8-eV reduced binding for the Cu $2s$ and $2p$ levels compared to the $d^{10}s^1$ free-atom case. Table III also shows estimated values for the cluster core-level shifts with this simplified approximation to screening. The results with screening are in fair agreement with the experimentally observed reduction of binding by 7.5 eV for bulk Cu core levels compared to free Cu core levels.

E. Trends with cluster size

1. Bonding charge distribution

In contrast to the DOS the total charge density is not very sensitive to cluster size. In order to com-

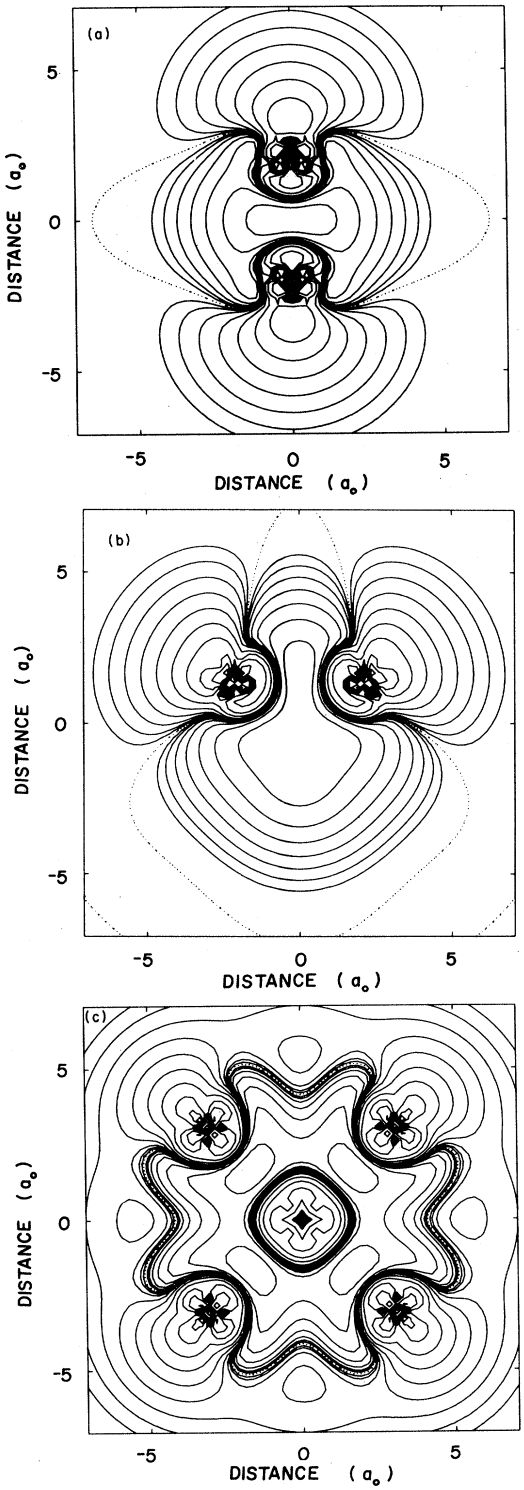

FIG. 2. Difference density $\Delta\rho=\rho$ (self-consistent field)$-\rho$ (overlapping atoms), with dotted contour at zero and full contours at $\pm(1,2,4,8,\ldots)\times10^{-4}e/a_0^3$. (a) Cu_2, (b) Cu_4 in a (110) plane; $\Delta\rho$ is positive at $r=(0,0,0)$; (c) Cu_{13} in a (100) plane; $\Delta\rho$ is positive in the interstitial region.

pare charge densities of the $Cu_2(D_{\infty h})$, $Cu_4(T_d)$, and $Cu_{13}(O_h)$ clusters, we have prepared charge-density difference plots where a reference density from overlapping atomic Cu densities is subtracted out. Such plots are shown in Fig. 2. For all three clusters the same pattern emerges: There is a depletion of charge in the core region and in the interstitial region the charge density is enhanced compared with overlapping atomic charge densities. Figure 2(a) shows the difference density for Cu_2. The enhancement of the charge density in the bond region can be seen clearly. In contrast to covalent bonds the region of enhanced charge density is much wider than the bond length. Figure 2(b) for the tetramer and Fig. 2(c) for the 13-atom cluster show enhanced charge density in the entire interstitial region.

2. *Binding energy versus bond length*

Figure 3 shows the binding-energy curves for Cu_2, $Cu_4(T_d)$, and $Cu_{13}(O_h)$ plotted versus nearest-neighbor separation. The curves show clearly that the equilibrium bond distance increases with increasing cluster size. The equilibrium binding energy per atom is also seen to increase with cluster size. At small bond length ($r<r_e$) the largest cluster shows the greatest repulsion. If there were a

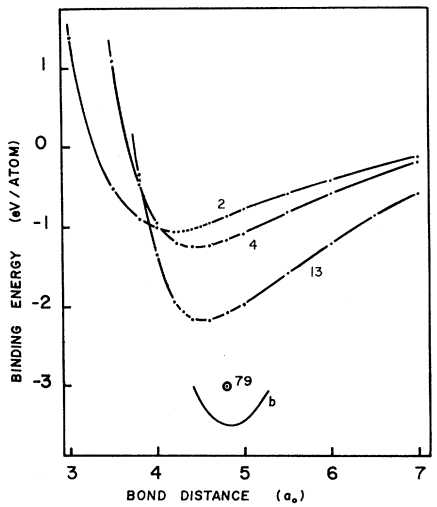

FIG. 3. Binding energy per atom for uniform scaling of the $Cu_2(D_{\infty h})$, $Cu_4(T_d)$, and $Cu_{13}(O_h)$ clusters vs bond distance. Calculated points are indicated by dots. The point ⊙ shows the binding energy of $Cu_{79}(O_h)$ with assumed bond distance equal to $4.8a_0$. The curve b denotes the bulk result obtained from experimental data for the cohesive energy, lattice constant, and bulk modulus.

universal pair potential for Cu, then the Cu_4 binding-energy curve should be scaled up by a factor of 1.5 from the Cu_2 curve, and Cu_{13} should be more attractive at all bond lengths. This is clearly not the case, so our density-functional-theory results cannot be reproduced by a single-Cu-pair potential. Figure 3 also shows that the binding-energy curves for uniform expansion of the cluster become increasingly steeper with increasing cluster size, thus implying an increase in the totally symmetric vibrational frequencies. In addition, we show in Fig. 3 a calculated point giving the cohesive energy of the Cu_{79} cluster for an assumed nearest-neighbor distance of $4.80a_0$, as well as an experimental curve derived from experimental lattice constants, cohesive energy, and bulk modulus. Since surface-relaxation effects in any cluster are expected to occur, which are not possible in bulk systems, we need to estimate their importance. Based on estimates from the Cu_{13} curve, one would expect that the surface shell contracts reducing the nearest-neighbor distance to the subsurface shell by not more than $0.25a_0$. With the use of the bulk and Cu_{13} curves for guidance less than a 0.1-eV increase in cohesive energy for the fully relaxed Cu_{79} cluster would be expected.

3. *Surface effects*

Cluster-size dependent quantities can be considered as surface effects. Thus the parameter $N^{-1/3}$, with N equal to the number of cluster atoms, is proportional to the surface-to-volume ratio if a fixed volume is associated with each atom in a spherical cluster. Figure 4 shows a plot of bond length versus this parameter. The theoretical equilibrium bond length shows a rather regular reduction upon going from the bulk to small clusters. This result is in qualitative agreement with the EXAFS study of Apai and co-workers,[2] who also find a monotonic reduction of bond length with decreasing cluster size. We have related their results to our parameter by assuming a constant atomic volume.

Figure 5 shows an even more linear trend of the local-density binding energy versus cluster size. The parameter $N^{-1/3}$ allows us to map all particle sizes from the single atom to the bulk into one picture. For $N^{-1/3}=1$ we have the isolated atom, which is the zero reference concerning cohesive energies. Note that the calculated dissociation energy of the dimer agrees very well with the experimental value and that our theoretical cluster binding energies extrapolate linearly to a bulk value of 4.0 eV.

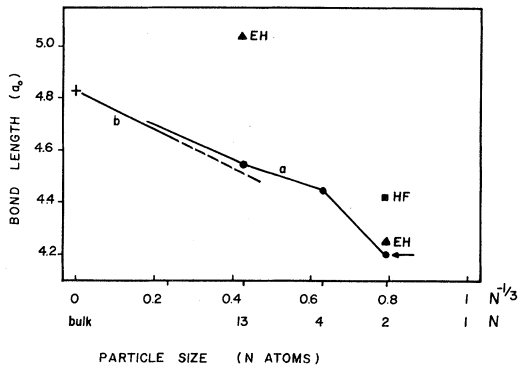

FIG. 4. Bond length versus particle size. The calculated local-density values, shown as ●, are connected by a solid curve labeled *a* for visual convenience and extrapolated linearly to the bulk theoretical-experimental value (+). The curve *b* is from the EXAFS data of Ref. 2 and its extrapolation. The arrow indicates the experimental value for the dimer, in excellent agreement with the calculated local-density value and the value from CI (Ref. 21). Results of other calculations are denoted as "EH" for extended-Hückel-theory results (Ref. 20). The result of a Hartree-Fock calculation is denoted by HF (Ref. 22).

(As discussed before, relaxation of the Cu_{79} could increase the extrapolated bulk cohesive energy to 4.1 eV.) This extrapolated bulk cohesive energy is, however, 17% larger than that observed experimentally, as is the value obtained from a bulk band-theory local-density calculation.[11] Indeed, it may be taken as reassuring evidence for the validity of the large-cluster approach that it yields an extrapolated bulk value that is close to that obtained for the cohesive energy by a totally independent Korringa-Kohn-Rostoker (KKR) bulk energy-band local-density method. Figure 5 also shows extended-Hückel-theory (EHT) results[20] for dimers, tetramers, and 13-atom clusters. For dimers an excellent prediction of the binding energy is obtained. However EHT cohesive energies decrease with increasing cluster size, which is against all expectations. Hartree-Fock (HF) results[22] are included in Fig. 5. The cohesive energy is consistently low for all the clusters considered. Despite the slight increase of the cohesive energy with increasing cluster size, it is difficult to see how bulk cohesive energies would be attained either with HF or with EH approaches.

Let us now focus on the surprising linearity of the cluster cohesive energy versus our parameter $N^{-1/3}$ seen in Fig. 5. This linearity implies that we can write for the cohesive energy per unit volume a simple relation

$$\epsilon_C=\epsilon_b-\frac{A}{V}\sigma \tag{9}$$

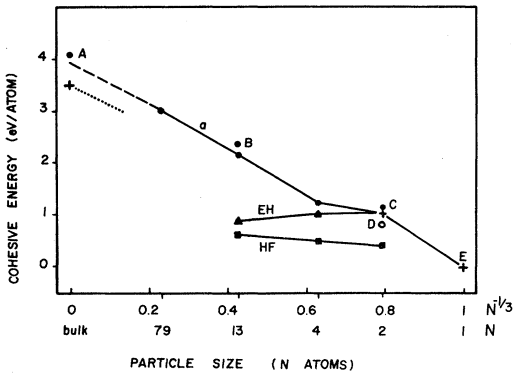

FIG. 5. Comparison of various results for the cohesive energy vs particle size (N is the number of atoms in the cluster and $N^{-1/3}$ is an effective surface-volume ratio). The experimental values for the atom, dimer, and bulk are indicated by a cross (+). The cross for the dimer coincides with the present $\alpha=0.7$ result and the extended-Hückel-theory (EH) result (Ref. 20). Point A is the bulk value obtained in Ref. 11 with the Hedin-Lundqvist potential; B is the cohesive energy for the 13-atom cluster with the same potential; C is the value for the dimer by Harris and Jones (Ref. 19) using the Gunnarsson-Lundqvist (GL) potential; it coincides with the present value for the GL potential; D is the value for the dimer by configuration-interaction theory (Ref. 21); E is the atomic binding energy, which is the zero reference for each method. The present result uses the spin-polarized atom $3d\uparrow^5 3d\downarrow^5 4s\uparrow^1$ configuration as the reference state. A line (a) connects the present $\alpha=0.7$ results. The extrapolation to bulk is discussed in the text. The line "EH" connects extended-Hückel-theory results (Ref. 20) and the line "HF" connects Hartree-Fock results (Ref. 22). The dotted line is taken from surface-tension data (Ref. 33).

to a good approximation, with ϵ_b the bulk cohesive energy per unit volume and a surface-tension contribution σ. If this equation is taken seriously then the surface tension can be calculated simply from the cohesive energy and the atomic volume: $\sigma \approx E_c(\text{bulk})/(4\pi r_{\text{ws}}^2)$ with the use of the Wigner-Seitz radius r_{ws}. Such estimates for the surface tension are shown in Table IV. It is obvious from the table that this simple linearity assumption applies fairly well to monovalent metals. We know that for divalent and polyvalent metals the cohesive energy does not scale linearly with $N^{-1/3}$. In divalent metals the surface tension is underestimated, and in polyvalent metals overestimated, by such an assumption of linearity.

4. *Sensitivity to exchange-correlation potential*

It is useful to compare predictions of the cohesive energy as obtained with different proposed forms of the effective exchange-correlation potential, as applied to the case of copper clusters. Table V shows a summary of the results obtained with the $\alpha=0.7$ $X\alpha$ potential as well as results obtained with the potential of Hedin-Lundqvist[28] (HL) and Gunnarsson-Lundqvist[29] (GL). It should be mentioned that the HL and GL potentials, which are very similar in structure, add Coulomb correlations not included in the simplest $X\alpha$ potential. The various potentials all yield the same electronic ground state (shown in the fifth column of Table V). The GL potential yields a cohesive energy for the dimer, which is 0.1-eV larger than that obtained from $X\alpha$. For the 13-atom cluster, a 10% increase (0.19 eV) in binding energy is obtained with the use of the HL potential.

Differences for the one-electron eigenvalues are more dramatic and amount to a shift of about 1 eV to higher binding energy with both the HL and GL potentials (cf. last column of Table V). Consequently, with HL or GL potentials, 1-eV higher ionization potentials would be predicted than are obtained with the $\alpha=0.7$ potential.

Finally, if one is willing to accept our extrapolated theoretical cohesive energy for bulk copper of 4.0 eV for the $\alpha=0.7$ potential (and 4.1 eV for the Hedin-Lundqvist potential), a reasonably clear picture emerges about the discrepancies between exper-

TABLE IV. Simple estimates for surface tension of selected metals [cf. Eq. (9)].

	σ_0 (exp)[a] (erg/cm^2)	σ (estimated) (erg/cm^2)	Deviation (%)
Li	463	480	+4
Na	236	219	−8
K	121	119	−2
Cs	83	98	+18
Cu	1583	1493	−6
Ag	1102	998	−10

[a]The experimental values have been extrapolated to zero temperature.

TABLE V. Numerical-basis and analytic-basis determinations of cohesive energy (E_c), ground-state one-electron energies of the highest occupied state ($-E_h$), and equilibrium bond lengths, r_e (in a.u.) for the different clusters studied. The potentials used are $\alpha=0.7$, GL (Gunnarsson-Lundqvist), and HL (Hedin-Lundqvist), as described in the text. For comparison we also cite the dimer results of Harris and Jones (Ref. 19) for Cu_2.

Cluster	Symmetry	Potential	State	E_c (ev/atom)	r_e (a.u.)	$-E_h$ (eV)
		Numerical basis				
Cu_2	$D_{\infty h}$	$\alpha=0.7$	$^1\Sigma_g^+$	1.05	4.20	4.35
Cu_4	T_d	$\alpha=0.7$	$^2T_2$	1.26	4.45	3.15
	$D_{\infty h}$	$\alpha=0.7$	$^1\Sigma_g^+$	1.23	center 4.40 outer 4.20	4.35
Cu_{13}	O_h	$\alpha=0.7$	$^2T_{2g}$	2.19	4.55	3.80
Cu_{79}	O_h	$\alpha=0.7$		3.03	fixed 4.8	3.65
Cu_2	$D_{\infty h}$	GL	$^1\Sigma_g^+$	1.15	fixed 4.25	5.40
Cu_{13}	O_h	HL	$^2T_{2g}$	2.38	fixed 4.50	4.70
		Analytical basis				
Cu_2	$D_{\infty h}$	$\alpha=0.7$	$^1\Sigma_g^+$	1.11	4.27	4.4
Cu_4	T_d	$\alpha=0.7$	$^2T_2$	1.21	4.6	2.43
		Harris and Jones				
Cu_2	$D_{\infty h}$	GL	$^1\Sigma_g^+$	1.15	4.30	5.4

imental and theoretical cohesive energies. It has been stated previously,[30] and is now generally accepted, that this discrepancy between theory and experiment is a result of local-spin-density approximations for the atom rather than on the bulk system, since the theory has been derived and is more appropriate for extended systems. In the case of Cu with its $3d^{10}4s^1$ configuration, atomic multiplet effects can be ruled out as a cause for the discrepancy. Following the discussion of cohesive energy versus our particle-size "surface" parameter $N^{-1/3}$, we first note that the theoretical binding energy for the Cu dimer agrees well with the experimental dissociation energy, being only slightly overbound. The smoothness of the trend of the cohesive energies with particle size shown in Fig. 5, extrapolated to give a bulk cohesive energy that is overbound by 0.5 eV, suggests that the error in the cohesive energy scales smoothly with the surface-to-volume ratio of the cluster. Hence the differential error from the surface term vanishes in the bulk limit and increases at the right-hand side of Fig. 5; thus we may consider the Cu atom to be underbound by half an electron volt. This suggests that local-density-theory predictions could be somewhat improved by adding a very small correction term to account for the inhomogeneity of the electron density in the atom. The remarkable success of the local-density approach for a variety of ground-state properties of bulk solids would then also extend to the calculation of cohesive energies.

ACKNOWLEDGMENTS

We would like to thank M. Weinert, E. Wimmer, and H. Jansen for enlightening discussions. This research was supported in part by the National Science Foundation Grant Nos. DMR79-25379 and DMR77-23776, and by NATO Grant No. 1826.

APPENDIX

For completeness we give some details of the binding-energy algorithm developed by Delley.[31] The total-energy estimate of local-spin-density theory is given by

$$E_t=\sum_\sigma \epsilon_{k,\sigma} n_{k\sigma}+\sum_\sigma \int \rho_\sigma(-\tfrac{1}{2}V_e-\mu_{\mathrm{xc},\sigma}+\epsilon_{\mathrm{xc}})d^3r+\tfrac{1}{2}\sum{}' \frac{Z_\mu Z_\nu}{r_{\mu\nu}} . \tag{A1}$$

We rewrite (A1) in the framework of the present variational approach as

$$\hat{E}(\rho_i)=\sum_{\sigma}\left[\sum_{k}\epsilon_{k,\sigma}n_{k,\sigma}-\tfrac{1}{2}\langle\rho_{i,\sigma}V_e(\rho_{i,\sigma})\rangle+\langle\rho_{i,\sigma}[\epsilon_{\rm xc}(\rho_i)-\mu_{{\rm xc},\sigma}(\rho_i^+,\rho_i^-)]\rangle\right]+\tfrac{1}{2}\sum{}'\frac{Z_\mu Z_\nu}{r_{\mu\nu}}\ , \tag{A2}$$

where k labels single-particle functions with eigenvalues ϵ_k and occupation $n(k)$. $\rho_{i,\sigma}$ is the spin density ($\sigma=+,-$) used to generate the effective potential.[14] V_e is the Coulomb potential due to the electrons, $\mu_{\rm xc}$ is an exchange-correlation potential [e.g., Eq. (3)] and $\epsilon_{\rm xc}$ is the corresponding energy density per electron. Eigenvalues $\epsilon_{k,\sigma}$ result from the variational solution of single-particle equations,

$$\sum_j\{[\langle-\tfrac{1}{2}\nabla^2+V_N+V_e(\rho_i)+\mu_{{\rm xc},\sigma}(\rho_i^+,\rho_i^-)\rangle_{ij}-\epsilon_{k,\sigma}\langle 1\rangle_{ij}]c_{j,k,\sigma}\}=0 \tag{A3}$$

with eigenvectors $\vec{c}_{k,\sigma}$. Here V_N is the nuclear Coulomb potential and $\langle f\rangle_{ij}$ denotes a linear sampling operator[32] approximating a three-dimensional integration of the type

$$\int\Phi_i(\vec{r})f(\vec{r})\Phi_j(\vec{r})d^3r \tag{A4}$$

with variational basis functions Φ_i.

The variational principle ensures that $\sum_{k,\sigma}\epsilon_{i,k,\sigma}n_{k,\sigma}$ is minimal for a given charge density ρ_i and for a given expansion set for the wave function $\{\Phi_i\}$, when $n_{k,\sigma}$ is chosen according to the Fermi distribution $n_{k,\sigma}=f(\epsilon_{k,\sigma})$. If we insert in Eq. (A2) the self-consistent density

$$\rho_i(r)=\rho_0(r)\equiv\sum n_{k,\sigma}\psi_k^*(r)\psi_k(r) \tag{A5}$$

with $\psi_k=\sum_j c_{j,k,\sigma}\Phi_j$, then the variational principle ensures, moreover, that $\hat{E}(\rho_0)$ is minimal with respect to variations in the $c_{j,k,\sigma}$. If ρ_i deviates from ρ_0, we observe that

$$\begin{aligned}\hat{E}(\rho_i)&=\hat{E}(\rho_0)+\sum_{k,\sigma}\delta\epsilon_{k,\sigma}n_{k,\sigma}+\delta[\tfrac{1}{2}\langle\rho V\rangle+\langle\rho(\epsilon_{\rm xc}-\mu_{\rm xc})\rangle]\\&=\hat{E}(\rho_0)+\langle(\delta V_e+\delta\mu_{\rm xc})\rho_0\rangle-\langle\rho_0\delta V\rangle\langle\rho_0\delta\mu_{\rm xc}\rangle+O((\delta\rho)^2)=\hat{E}(\rho_0)+O((\delta\rho)^2)\ .\end{aligned} \tag{A6}$$

Thus we show that first-order corrections to $\hat{E}$ vanish by using

$$\delta\langle\rho V_e(\rho)\rangle=\langle V_e(\rho)\delta\rho\rangle+\langle\rho\delta V_e(\rho)\rangle=2\langle\rho\delta V_e(\rho)\rangle+O((\delta\rho)^2)$$

and the relation $\delta[\rho\epsilon_{\rm xc}(\rho)]=\mu(\rho)\delta\rho$, with $\delta\rho=\rho_i-\rho_0$ and $\delta V(\rho_0)=V(\rho_i)-V(\rho_0)$. Thus we have shown that $\hat{E}(\rho_i)$ in (A2) is stationary versus differences $\delta\rho=\rho_i-\rho_0$ as well as versus variations of the eigenvectors. The Rayleigh-Ritz theorem ensures that $E\geq E_0$. The lower bound E_0, however, need not be equal to the local-density ground-state energy because of the use of a linear sampling operator. We recall in passing that one-electron eigenvalues are affected to first order by $\delta\rho$, as expected.

A further important element of numerical noise reduction for molecular binding-energy calculations can be introduced by realizing that (A2) equals

$$\begin{aligned}\hat{E}(\rho_i)&=\left\langle\sum_{k,\sigma}\epsilon_{k,\sigma}n_{k,\sigma}\psi_k^*\psi_k+\sum_{\sigma}[-\tfrac{1}{2}\rho_{i,\sigma}V_e+\rho_{i,\sigma}(\epsilon_{\rm xc}-\mu_{{\rm xc},\sigma})]\right\rangle+\tfrac{1}{2}\sum{}'\frac{Z_\mu Z_\nu}{r_{\mu\nu}}\\&=\langle e(\vec{r})\rangle+\tfrac{1}{2}\sum{}'\frac{Z_\mu Z_\nu}{r_{\mu\nu}}\ ,\end{aligned} \tag{A7}$$

where $e(\vec{r})$ is an energy density. We wish to suppress numerical noise arising from the first term in (A7) in evaluating binding energies:

$$\hat{E}_b=\hat{E}_t-\hat{E}_t^{\rm ref}\ , \tag{A8}$$

with $\hat{E}_t^{\rm ref}$, the energy of the separated atoms, as our standard reference. Subtraction of this constant can be taken inside the approximate three-dimensional integration as

$$\hat{E}_b=\langle e(\vec{r})-e^{\rm ref}(\vec{r})\rangle+\tfrac{1}{2}\sum{}'\frac{Z_\mu Z_\nu}{r_{\mu\nu}}\ . \tag{A9}$$

This leads to stable convergence of $\hat{E}_b$ versus quality of expansion basis for both $\{\Phi_i\}$ and ρ_i. Numerical studies on the convergence of the linear sampling operators show that present cohesive-energy values are converged to better than 10^{-2} eV/atom.

[1]F. W. C. Boswell, Proc. Phys. Soc. London, Sec. A 64, 465 (1951).

[2]G. Apai, J. F. Hamilton, T. Stohr, and A. Thompson, Phys. Rev. Lett. 43, 165 (1979).

[3]H. G. Mason and R. C. Baetzold, J. Chem. Phys. 64, 271 (1976).

[4]M. Moskovits and J. E. Hulse, J. Chem. Phys. 67, 4271 (1977).

[5]N. Ashlund, R. F. Barrow, W. G. Richards, and D. N. Travis, Ark. Fys. 30, 171 (1965).

[6]B. Kleeman and S. Lundqvist, Ark. Fys. 8, 333 (1954).

[7]For example, extended-Hückel-theory calculations on Ag_n clusters are presented by R. C. Baetzold, J. Chem. Phys. 62, 1513 (1975); also see Ref. 20.

[8](a) Hartree-Fock calculations have been made on clusters such as Ni_6 [H. Basch, M. D. Newton, and J. W. Moskowitz, J. Chem. Phys. 73, 4492 (1980)] and as large as Cu_{13} (see Ref. 22). However, because of the rapid growth in the number of two-electron integrals, such calculations are usually carried out using very restricted basis sets; (b) The Hartree-Fock-Slater or $X\alpha$ method is described by J. C. Slater, in *The Self-Consistent Field for Molecules* (McGraw-Hill, New York, 1974). A review of the accuracy of one-electron and ground-state properties obtained by local-density methods *vis-à-vis* experiment and HF models is given in Ref. 12.

[9]Of particular relevance here are the recent GVB—van der Waals calculations on Mo_2 and Cr_2: M. M. Goodgame and W. A. Goddard III, Phys. Rev. Lett. 48, 135 (1982).

[10](a) T. Ziegler and A. Rauk, Theor. Chim. Acta 43, 261 (1977); (b) U. von Barth, Phys. Rev. A 20, 1693 (1979).

[11]V. L. Moruzzi, J. F. Janak, and A. R. Williams, *Calculated Electronic Properties of Metals* (Pergamon, New York, 1978).

[12]O. Gunnarsson and B. I. Lundqvist, Phys. Rev. B 13, 4274 (1976).

[13]For a comparative review of HFS-STO calculations up to 1978, see E. J. Baerends and P. Ros, Int. J. Quantum Chem. Suppl. 12, 169 (1978).

[14]E. J. Baerends, D. E. Ellis, and P. Ros, Chem. Phys. 2, 41 (1973); E. J. Baerends and P. Ros, *ibid.* 2, 52 (1973).

[15]B. Delley and D. E. Ellis, J. Chem. Phys. 76, 1949 (1982).

[16]D. Post, Ph.D. thesis, Free University, Amsterdam, 1981 (unpublished); D. Post and E. J. Baerends, Chem. Phys. Lett. 86, 176 (1982), and unpublished.

[17]B. Delley (unpublished). For O_2 ($d=2.282$ a.u.) the binding energy vs spin-polarized atoms increases from 1.19 eV for a minimal basis to 4.24 eV with double basis and to 5.49 eV with the inclusion of d-polarization functions.

[18]K. Gingerich, J. Cryst. Growth 9, 31 (1971).

[19]J. Harris and R. O. Jones, J. Chem. Phys. 70, 830 (1979).

[20]A. B. Anderson, J. Chem. Phys. 68, 1744 (1978).

[21]P. Joyes and M. Leleyter, J. Phys. B 6, 150 (1973).

[22]C. Bachmann, J. Demuynck, and A. Veilland, Faraday Symp. Chem. Soc. 14, 170 (1980).

[23]J. O. Noell, M. D. Newton, P. J. Hay, R. L. Martin, and F. W. Bobrowicz, J. Chem. Phys. 73, 2360 (1980).

[24]It is well known that a change in E_t of Eq. (6) is second order with respect to a variation in the density ρ. Manipulation of Eqs. (6) and (7) reveals that variations of the binding energy E_b are also of second order, provided that the separated-atoms limit is treated exactly. See the Appendix for details.

[25]J. A. Appelbaum and D. R. Hamann, Solid State Commun. 27, 881 (1978).

[26]H. von Laue, Ann. Phys. (Leipzig) 44, 1197 (1914).

[27]P. H. Citrin, G. K. Wertheim, and Y. Baer, Phys. Rev. Lett. 41, 1425 (1978).

[28]L. Hedin and B. I. Lundqvist, J. Phys. C 4, 2064 (1971).

[29]O. Gunnarsson, B. I. Lundqvist, and S. Lundqvist, Solid State Commun. 11, 149 (1972).

[30]W. Kohn, in *Energy Bands in Metals and Alloys,* edited by L. H. Bennet and T. M. Waber (Gordon and Breach, New York, 1968), p. 65.

[31]B. Delley (unpublished).

[32]D. E. Ellis and G. S. Painter, Phys. Rev. B 2, 2887 (1970).

[33]Yu. V. Naidich and V. N. Eremenko, Fiz. Met. Metalloved. 11, 883 (1961).